Radiologic imaging of the inflammatory renal diseases: literature review

Ruta Pupalyte[1], Algidas Basevicius[2]

[1] *Faculty of Medicine, Lithuanian University of Health Sciences, Kaunas, Lithuania,*
[2] *Department of Radiology, Lithuanian University of Health Sciences, Kaunas, Lithuania*

ABSTRACT

Background and aim: Inflammatory diseases of the kidney are a broad group of various renal pathologies. They are usually recognized by clinical symptoms and laboratory tests. However, radiology also has a role. The aim of this article is to assess radiologic imaging possibilities in diagnosis and follow-up of the most common inflammatory renal diseases.

Materials and methods: A selective search was carried out for relevant studies regarding radiologic imaging of acute pyelonephritis, renal and perinephric abscesses, emphysematous pyelonephritis, emphysematous pyelitis, chronic pyelonephritis and glomerulonephritis. ClinicalKey, Cochrane Library, Medline (PubMed), ScienceDirect and SpringerLink databases were used.

Results: Ultrasound is usually used as the initial imaging tool to evaluate patients with symptoms of acute pyelonephritis. However, computed tomography is the most appropriate imaging modality. If an abscess or gas-forming infection are suspected, CT is the modality of choice. The findings characteristic, yet not pathognomic to chronic pyelonephritis can be assessed using all of the previously mentioned imaging tools. In cases of glomerulonephritis, US and MRI are the most suitable.

Conclusion: Radiology plays an important role in diagnosis of inflammatory renal diseases. Imaging allows to identify renal abnormalities and differentiate between a few feasible pathologies. It may also evaluate the activity of the disease. Moreover, it can assess sequelae, such as renal scarring and decreased renal function.

Keywords: pyelonephritis, renal abscess, glomerulonephritis, ultrasound, computed tomography, magnetic resonance imaging.

1. INTRODUCTION

Inflammatory diseases of the kidney are a broad group of various renal pathologies. These diseases can be insintric or manifest as systemic illnesses. The etiology of inflammation may be diverse, e.g. infectious or autoimmune. Inflammatory diseases are usually recognized by clinical symptoms and laboratory tests, such as blood count, C-reactive protein, autoantibodies and urinalysis [1, 2]. In some cases, percutaneous renal biopsy is the sole method that can confirm the diagnosis. However, it is an invasive procedure with potential complications [3].

Therefore, radiology also plays a role in the diagnosis. Radiologic imaging is constantly evolving and more new techniques emerge. With a wide variety of renal imaging tools, it is important to choose the modality which would provide the most information about the nature and extent of inflammatory lesions.

2. AIM

To assess radiologic imaging possibilities in diagnosis and follow-up of the most common inflammatory renal diseases.

3. MATERIALS AND METHODS

A selective search was carried out for relevant studies regarding radiologic imaging of acute pyelonephritis (APN), renal and perinephric abscesses, emphysematous pyelonephritis (EPN), emphysematous pyelitis (EP), chronic pyelonephritis (CPN) and glomerulonephritis (GN). We selected databases from the subscription list of Lithuanian University of Health Sciences. ClinicalKey, Cochrane Library, Medline (PubMed), ScienceDirect and SpringerLink databases were used.

4. RESULTS

Intravenous urography (IVU) has been replaced

almost completely by other modalities in diagnosis of APN, although this imaging technique was commonly performed in the past.

Ultrasound (US) is used as the initial imaging tool to evaluate patients with symptoms of APN. However, examination is usually normal due to relatively low sensitivity and specifity of this modality [4].

Computed tomography (CT) is the most appropriate imaging modality for diagnosing APN and its complications [5–8]. CT can also be useful in predicting the clinical course of the disease [9–11].

Magnetic resonance imaging (MRI) is not commonly used in diagnosing acute renal infections. Nonetheless, it is a radiation-free alternative for those patients who should not be exposed to radiation or are allergic to iodinated contrast agents.

Renal cortical scintigraphy (RCS) has high sensitivity in diagnosing renal infection [5, 12, 13]. RCS is considerably superior to IVU and US [14], as reliable as CT [5] and inferior to enhanced MRI [15] and DWI-MRI [16] in the acute phase of APN. Planar RCS is also slightly inferior or equivalent to single photon emission computed tomography (SPECT) in detecting pyelonephritic lesions [13, 17, 18].

If renal or perinephric abscess is suspected, CT is the modality of choice [19, 20]. MRI is not a frequently used imaging technique. US is inferior to CT and MRI in diagnosing renal abscesses [21].

US underestimates the depth of parenchymal involvement and perinephric extention of emphysematous pyelonephritis [22]. Therefore, CT is the most reliable imaging modality [23, 24].

Findings characteristic, yet not pathognomic to chronic pyelonephritis can be assessed using all of the above mentioned modalities. However, CT and MRI depict these findings in more detail. In cases of glomerulonephritis, US and MRI are the most appropriate imaging tools.

Figure 1. Bilateral focal acute pyelonephritis. Axial contrast-enhanced CT depicts a few hypodense wedged-shaped pyeonephritic lesions in both kidneys. (Wang JH. Acute focal pyelonephritis. Urol Sci 2013; 24: 56-57)

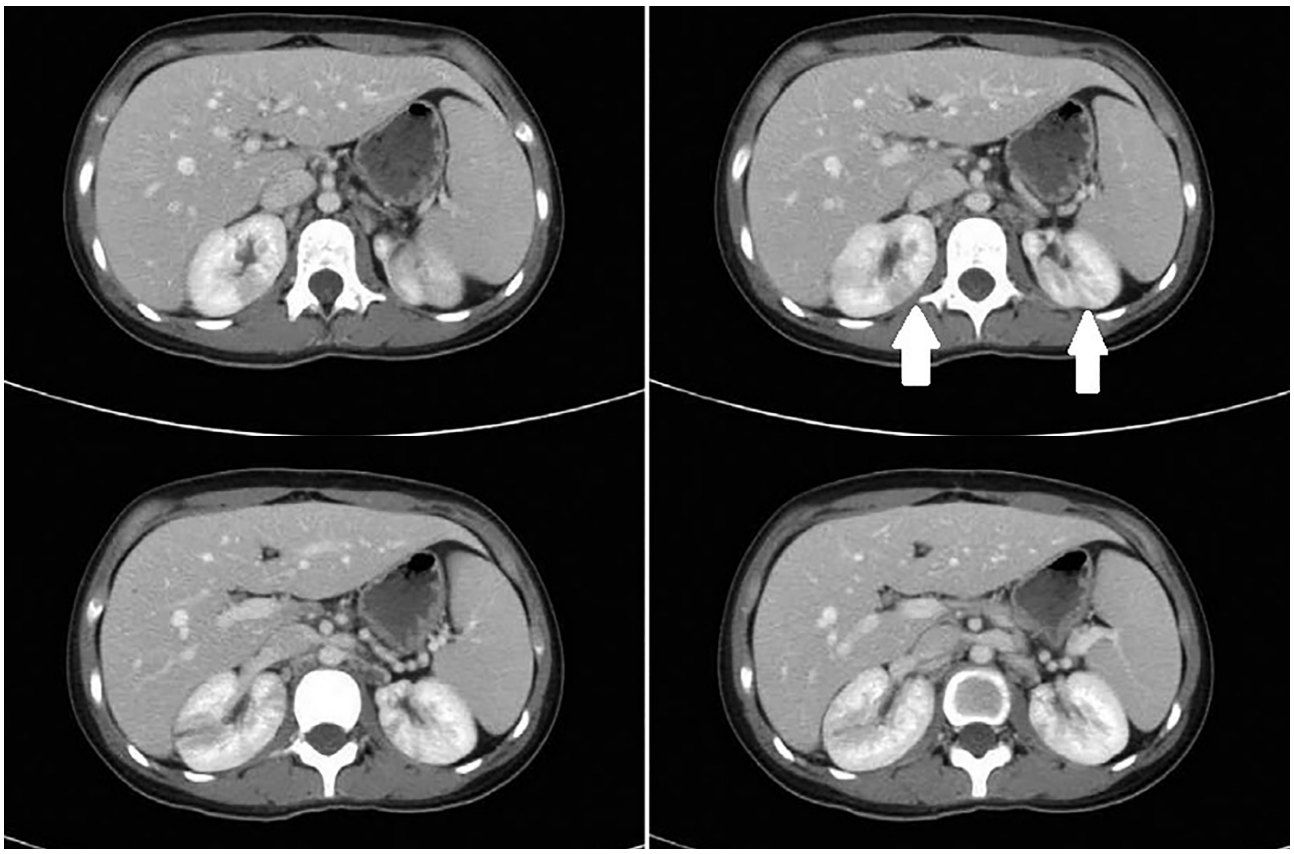

Figure 2. Renal abscess. A well-defined hypodense lesion with peripheral enhancement is observed on coronal contrast-enhanced CT scan. (Linder BJ, Granberg CF. Pediatric renal abscesses: a contemporary series. J Pediatr Urol 2016; 12: 99.e1-99.e6)

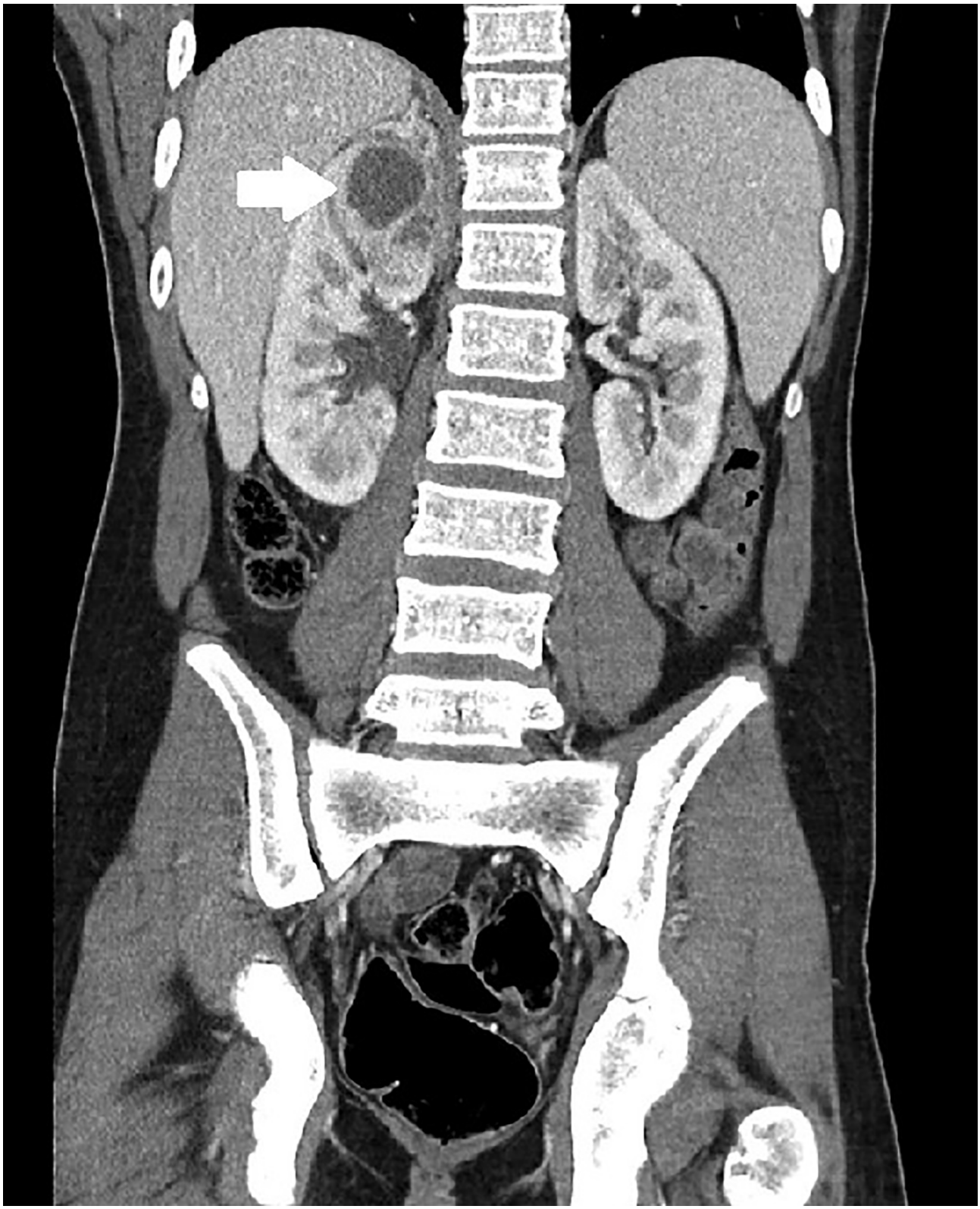

Figure 3. Emphysematous pyelonephritis. Native CT shows enlarged bilateral kidneys with gas collections in the renal parenchyma. (Yao J, Gutierrez OM, Reiser J. Emphysematous pyelonephritis. Kidney Int 2007; 71: 462-465)

Figure 4. Emphysematous pyelitis. Gas in the bilateral pelvises and ureters (arrows) is observed on coronal native CT scan. Also, gas is seen in the left ureterovesicular junction (arrowhead). Asterisks show fat stranding. (Wiesel S, Hutman A, Abraham JE, Kiroycheva M. Foley follies: emphysematous pyelitis from instrumentation in obstructive uropathy. Cureus 2017; 9: e1612)

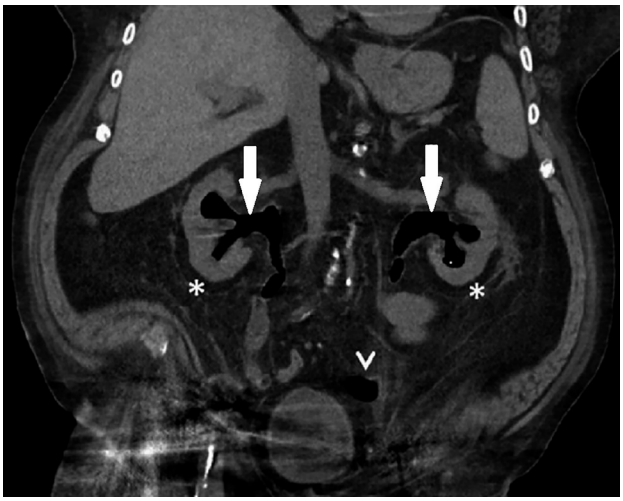

Figure 5. Chronic pyelonephritis. On US, the right kidney is apparently smaller than the left one 7.6 cm vs. 11.5 cm). The renal parenchyma is echogenic and thin. Hypertrophy of the left kidney is observed. (Paltiel HJ, Babcock DS. The pediatric urinary tract and adrenal glands. In: Rumack C, Levine D. Diagnostic ultrasound. 5th ed. Philadelphia, PA, USA: Elsevier; 2018. pp. 1775-1832)

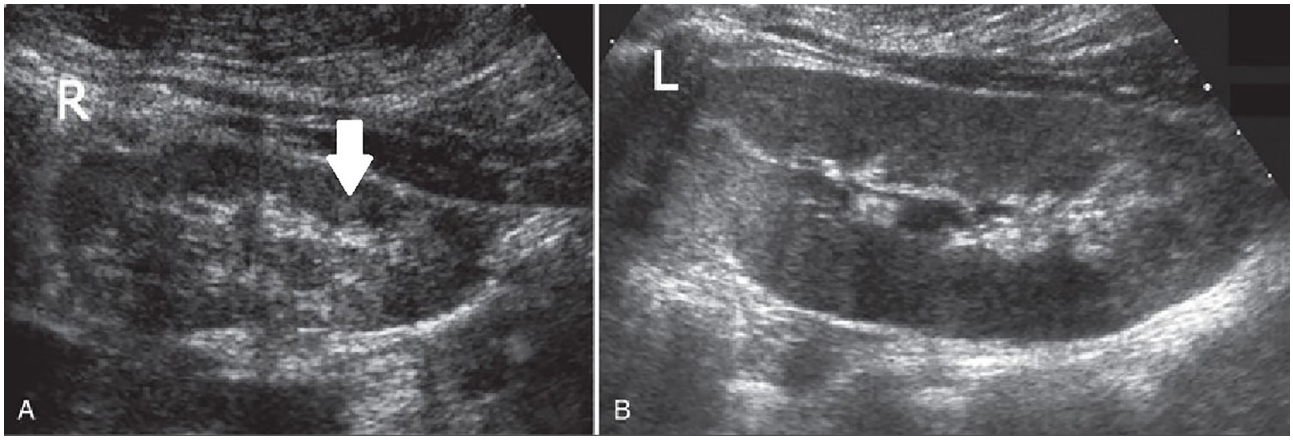

Figure 6. Chronic pyelonephritis. Axial (a) and coronal (b) contrast-enhanced CT demonstrates scarring with cortical retraction (arrows) and calyceal deformation characteristic to CPN. (Ifergan J, Pommier R, Brion MC, Glas L, Rocher L, Bellin MF. Imaging in upper urinary tract infections. Diagn Interv Imaging 2012; 93: 509–519)

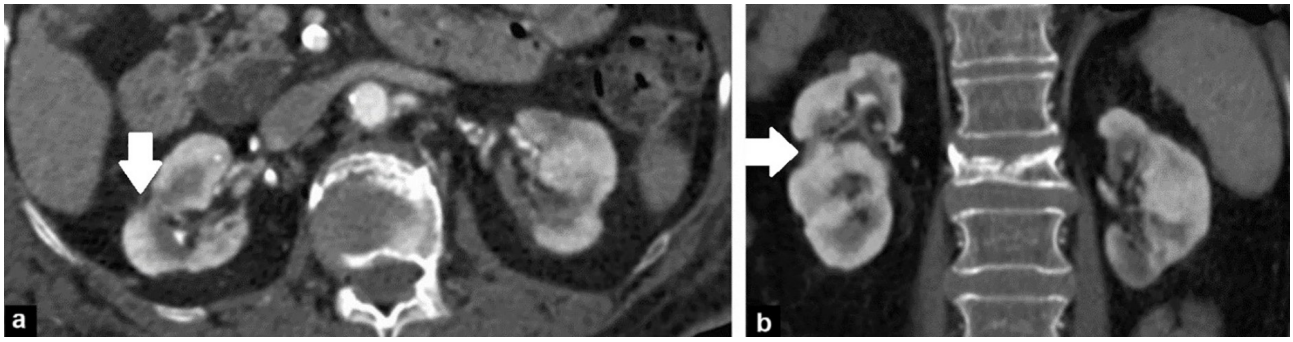

Figure 7. Chronic glomerulonephritis. ADC maps (a-e) and FA maps (f-j) are shown in different disease stages (1-5) using MRI-DTI. Low signal region of the renal medulla on ADC maps and high signal region on FA maps decreases with each stage. Loss of corticomedullary differentiation is also apparent with increased stages. (Feng Q, Ma Z, Wu J, Fang W. DTI for the assessment of disease stage in patients with glomerulonephritis - correlation with renal histology. Eur Radiol 2015; 25: 92–98)

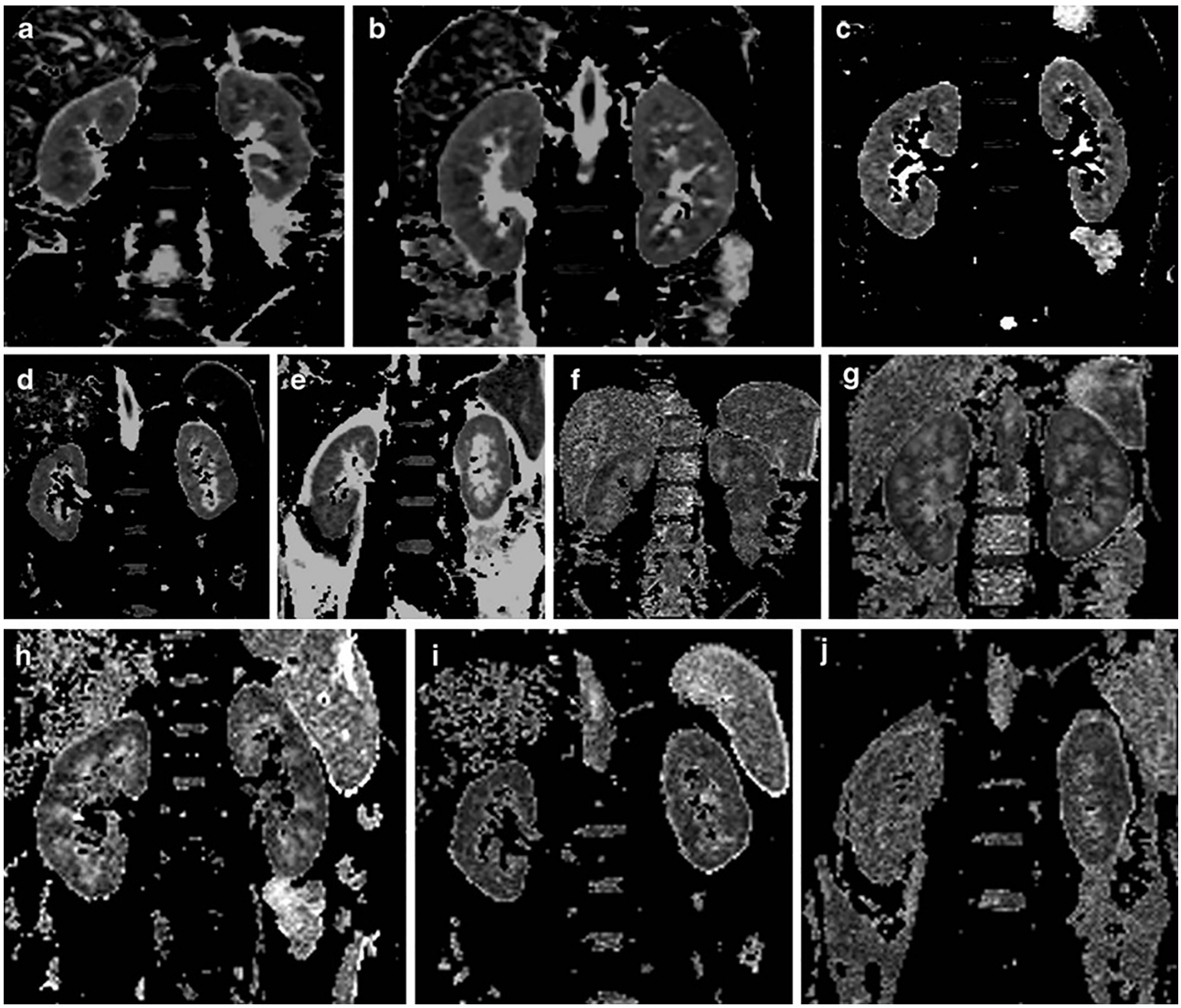

5. DISCUSSION

APN is an inflammation of the renal parenchyma and collecting system. Incidence rates of APN are highest in young females, infants and the elderly population [25, 26]. The most frequent causative uropathogen is Escherichia coli (70-80%) [25]. In most cases, APN is unilateral [27]. Diagnosis of APN is based on clinical and laboratory findings, therefore, radiologic imaging is not routinely used. However, diagnostic imaging allows to exclude urgent urinary pathologies.

In approximately 75% cases of uncomplicated APN, IVU is normal [14].

Abnormal findings characteristic to acute renal infection are diffuse renal enlargement, striated or delayed renal nephrogram and effacement or dilatation of the collecting cavities with delayed contrast medium filling [14]. Papillary necrosis, one of the possible complications of APN, can also be diagnosed on IVU [28].

Excretory urography is useful for assessment of the pelvocalyceal anatomy, however, it visualizes the renal parenchyma poorly [29].

On conventional US (CUS), generalised edema of the afftected kidney, loss of corticomedullary differentiation, pelvicalyceal thickening and dilatation without any evident obstruction are typical features of diffuse APN [4, 14, 30]. Hyperehoic perirenal fat, implying inflammatory response of the adjacent tissue, is also suggestive of diffuse APN.

In cases of focal APN, wedge-shaped or round hyper-, iso- or hypoechoic areas with regional loss of corticomedullary differentiation can be seen in the renal parenchyma [4, 14, 31, 32] These abnormal mass-like areas can be of low attenuation and have indistinct margins [33, 34]. Therefore, differentiation from renal abscess and tumours is important.

As a result of APN, renal scarring can develop, especially in patients with vesicoureteral reflux or recurrent infection [35]. On CUS, irregular contour, focal parenchymal thinning and underlying calyceal deformation are indicative of scars caused by previous infection [36–38].

The additional use of color or power Doppler increases sensitivity of CUS in diagnosis of focal APN [39, 40]. These imaging techniques present pyelonephritic lesions as hypovascular or even avascular foci [41–43].

However, several studies established that contrast-enhanced ultrasonography (CEUS) displays parenchymal abnormalities, associated with APN, better [44, 45]. Characteristic to focal APN, wedge-shaped or round hyperechoic lesions are hypoenchancing during the cortical and early parenchymal phase, isoenchancing and then hypoenchancing in the late parenchymal phase [43, 46]. These CEUS findings allow to exclude the growth of an abscess if a patient is unresponsive to antibiotic therapy. Nonetheless, using contrast enhancement in evaluating the affected kidney has not yet become the general practise because it does not significantly improve the accuracy of US [47].

Lastly, more recent techniques, such as tissue harmonic imaging (THI) and pulse inversion harmonic imaging (PIHI), has become valuable in abdominal imaging. These techniques provide higher spatial resolution. According to Kim et al., THI and PIHI, whether or not contrast material is used, are superior to CUS in the detection of focal pyelonephritic lesions [34].

Multiphasic helical CT protocol allows to evaluate kidneys accurately for APN [48]. Non-contrast CT may appear without any abnormal findings in patients with diffuse APN. It can also demonstrate only secondary signs of renal infection, such as low-attenuation renal parenchyma [49], general renal enlargement, pelvocalyceal thickening and enhancement, soft tissue perinephric stranding and thickening of the anterior pararenal (Gerota's) fascia [28, 50]. If radiologic imaging is performed early, wall thickening of the pelvis and calyces can be the only feature of the disease [48].

On native CT scans, focal APN presents in a different manner. Involved areas usually appear oval or wedge-shaped, ill-defined and hypodense owing to edema or necrosis [7, 21, 49, 50]. In rare cases of haemorrhagic focal APN, non-contrast CT shows hyperdense lesions due to parenchymal bleeding [32]. Therefore, abnormal density of renal lesions on CT correspond to echogenicity on CUS [7, 32]. Focal pyelonephritic lesions have a lobular distribution, contrary to renal abscesses. If a CT scan presents with round, not

wedge-shaped low attenuation peripheral renal lesions in a patient displaying symptoms of APN, hematogenous seeding should be considered.

A recent study demonstrated association of focal APN to atypical radiological findings. Pleural effusion, presence of fluid around the gallblader, thickened gallblader wall, perinephric fluid and ascites are more frequent in patients with focal form of APN [51].

Postcontrast CT examination commonly shows solitary or multiple wedge-shaped zones of low attenuation extending from the papilla to the cortical surface with poor corticomedullary differentiation (Figure 1). Enhancement of abnormal areas is inhomogeneous, delayed and only moderate, always less than of unaffected parenchyma [7, 42, 50, 52]. Moreover, sharply defined alternating bands of increased and decreased attenuation („striations") within the wedge-shaped lesions can be observed during nephrographic phase [47]. These uni- or multifocal lobular striations are the result of tubular stasis of contrast material due to inflammatory tubular obstruction [53]. However, „striated nephrogram" is characteristic, but not pathognomonic of APN. It may also be observed in cases of contusion, renal vein thrombosis, ureteric obstruction and dehydratation [54].

CT can promptly lead to the diagnosis of APN. However, it should be preserved for patients with history of diabetes mellitus, renal calculi or renal surgery and those who are unresponsive to antibiotic therapy after 72 hours.

MRI findings of APN are similar to those of CT. The affected kidney is focally or diffusely enlarged with poor corticomedullary differentiation and typical heterogeneous edematous lesions, i.e., low signal intensity (SI) on T1-weighted (T1W) images and high SI on T2-weighted (T2W) images [55, 56]. These edematous areas are better represented using T2W images with fat supression technique [48]. Perirenal effusion, stranding and pelvocalyceal wall thickening can be found, but these signs are not pathognomic to APN [48, 55].

Renal scarring, a sequela of APN, appears as a contour deformity without signal change [15].

MRI with gadolinium depicts renal lesions as wedge-shaped or round, sometimes striated regions of decreased or absent enhancement [56]. Inversion recovery MRI with gadolinium uses the negative enhancement effect of the contrast material. Unaffected renal parenchyma becomes hypointense, contrary to the inflammatory areas that remain hyperintense due to edema and poor delivery of the contrast medium [15].

However, T1W and T2W images are not sensitive enough to detect pyelonephritic lesions [56]. Various studies reveal the utility of diffusion weighted imaging (DWI) in cases with suspected APN. According to De Pascale et al., sensitivity and specificity of DWI-MRI is 95.2% and 94.9%, respectively [55]. On DWI, APN presents as areas of restricted diffusion, corresponding to the T1W and T2W parenchymal signal changes. Pyelonephritic lesions are hyperintense. Reduced SI is seen on apparent diffusion coefficient (ADC) maps [55, 57, 58]. DWI displays high diagnostic agreement with gadolinium-enhanced images [55, 57]. Moreover, DWI does not require contrast medium, hence, it can be used in patients with renal insufficiency or pregnant women. Therefore, unenhanced MRI with DWI should be a comprehensive examination in diagnosing APN [55, 57].

MR urography (MRU) allows to assess the urinary tract for obstruction which may predispose APN [59, 60]. Thus, the combination of conventional MRI and MRU is appropriate to evaluate renal infection, its complications and the urinary tract for dilatation. Furthermore, conventional MRI together with MRU allows to obtain morphologic and functional data and eliminates the need for renal scintigraphy, especially in children [61, 62].

There is no general agreement for the use of RCS in diagnosis of pyelonephritis. In pediatric population, clinical and laboratory findings frequently do not correlate to RCS, thus, RCS is important in diagnosis of APN [63]. Nevertheless, it is not recommended in routine practice [64, 65].

Several tracers are available, although 99mTc-dimercaptosuccinic acid (99mTc-DMSA) is the most appropriate. The uptake of 99mTc-DMSA correlates to the volume of functioning renal parenchyma. In patients with APN, scintigraphy usually displays reduced focal or diffuse build-up of the radiopharmaceutical without cortical

or volume loss [12, 15, 17]. Relative left and right 99mTc-DMSA uptake can be measured, normal lowest value being 45%. In cases of APN, relative uptake can be decreased [12]. These findings are not specific to the disease, hence, combination of RCS and other imaging modalities should be used.

RCS is also used for detecting the consequences of APN [16, 66, 67]. In adult patients, renal scarring is rare, therefore, RCS examination is more frequent in children. In 42% of pediatric population, persistent cortical abnormalities are found [68]. Normal RCS scans during the acute phase of APN show a low risk of scarring later [69]. Scars present as defects in uptake with cortical thinning and loss of volume in the same area as pyelonephritis [16]. Inflammatory parenchymal changes tend to dissapear only after a few months after the episode of APN [70]. In order to assess possible sequelae, it is recommended to undergo scintigraphy for pediatric patients at least 6 months after APN [65].

Renal abscess is a collection of pus limited to the kidney. In most cases of APN, patients do not experience this complication. However, if inflammation is severe, liquefarctive necrosis and, consequently, abscess can form. Several studies show that renal abscesses are more common in patients with diabetes mellitus and urolithiasis [19, 71]. Clinical and laboratory findings cannot identify patients with or without abscesses, therefore, radiologic imaging is important [21, 72].

In most cases of acute renal abscess, the kidney is enlarged with distorted outer contour. The abscess itself presents as a hypoechoic mass with through transmission and hazy borders [43, 52, 73, 74]. A fluid-filled mass with a thickened definite margins suggests a mature abscess [48]. Mobile debris can be observed inside the collection of pus [74]. On power Doppler, absent internal flow is seen [43].

Depiction of abscesess is better using THI and PIHI than CUS [34].

CEUS may demonstrate round unenhanced abscess cavities with possible rim or septa enhancement which allows to differentiate it from focal APN [43]. Nevertheless, US is inferior to CT and MRI in diagnosing renal abscesses [21].

Liquefaction of affected region is seen as a hypoattenuating area in the peripheral cortex on unenhanced CT [52].

Contrast-enhanced CT shows early renal abscess as a round hypodense well-defined fluid-filled area with an irregular wide halo of decreased enhancement, as shown in Figure 2 [74–77]. The outer contour of capsule can be irregular owing to surrounding inflammatory infiltration. Septations and areas of gas may also be observed within a suppuration [74], the latter being pathognomonic of an abscess. Secondary features of infection, such as thickening of Gerota's fascia, can also be found [52].

Collections of pus may be also observed in perinephric spaces [52]. Perinephric suppuration usually originates from ruptured renal cortical abscesses into the pararenal space. Furthermore, it can involve the muscles of the posterior abdominal wall, most frequently the psoas muscle. Hypodense mass with indistinct borders, gas bubbles or air-fluid levels in the enlarged psoas muscle leads to diagnosis of abscess [75, 78].

MRI is used as a substitute when CT scans cannot be performed. In cases of suppuration, MRI shows round inhomogenous hypointense lesions with thick walls on T1W images and hyperintense lesions with hypointense periphery on T2W images [56, 57].

Gadolinium-enhanced MRI scans display unenhanced areas, surrounded by high SI peripheral rim [56, 76]. Cellular debris and irregular septations can also be seen within the abscess. Edema or fine streaks of fluid can be found in the perirenal space [56].

On DWI-MRI, inflammatory changes are hyperintense with restricted ADC [57, 79].

EPN is a rare life-threatening, usually fulminant urologic infection with gas accumulation within or around the kidneys. Emphysematous pyelitis (EP) is a less severe gas-forming renal infection with gas limited only to the renal collecting system. However, mortality between patients with EPN and EP does not significantly differ [80]. Uropathogens, such as E. coli, Klebsiella, Proteus, use the necrotic tissue as a substrate to produce carbon dioxide, thus, gas formation is seen. EPN and EP are more common in female patients [22, 23, 80–83]. These diseases are usually

unilateral [22, 23, 80, 81]. Uncontrolled diabetes mellitus and urolithiasis are associated with EPN [23, 81, 84].

Abdominal radiograph can display mottled gas shadows over the renal fossa, which should not be mistaken for bowel gas [85, 86]. If EPN progresses, speckled or crescent-shaped gas collection can be seen. Calculi may be observed as well [23].

CUS shows an enlarged kidney with parenchymal or pelvocalyceal hyperechoic foci with posterior dirty acoustic shadowing that are characteristic of gas [85].

In cases of EPN, native CT detects the presence and extent of gas in the renal parenchyma and around the kidney, possible accumulation of perinephric fluid, abscesses, along with the origin of obstruction if present [86]. Intraparenchymal gas appear as small bubbles or fine streaks of air radiating from papillae on native CT (Figure 3). Contrast-enhanced CT may show irregular enhancement or delayed excretion [48].

Wan et al. characterized two types of EPN based on CT findings. Type 1 exhibits focal tissue necrosis with mottled or loculated gas collections in the renal parenchyma or collecting system. Gas can extend to the subcapsular, perinephric and pararenal spaces. In type 2, these features are accompanied by renal or perirenal fluid collections. Type 1 is more aggresive and, consequently, has a higher mortality rate than type 2 (69% vs. 18%) [87].

Huang et al. classified EPN into several classes according to CT. Class 1 presents only pelvocalyceal gas, class 2 is distinguished by parenchymal gas, in class 3A abscess or gas are extended to perinephric space, in class 3B extension is seen in pararenal space. Class 4 represents bilateral EPN [88].

These classifications allow to predict the course of EPN and apply the most appropriate treatment [22].

The lack of intraparenchymal gas differentiates EP from EPN [89]. In cases of EP, non-contrast CT demonstrates bubbles of gas or gas-fluid levels in the collecting system and pelvic or calyceal dilatation, as seen in Figure 4.

CPN is a chronic tubulointerstitial fibrosing nephritis that involves renal parenchyma and the collecting system. The purpose of radiologic imaging is to detect not only chronic renal damage, but also the underlying cause of the recurrent inflammation.

In cases of CPN, IVU usually shows focal contraction of the renal parenchyma with adjacent calyceal clubbing [90, 91]. However, this modality is not so commonly used.

On US, may display focal or diffuse renal atrophy, hyperechoic parenchyma, irregular contour, loss of corticomedullary differentiation and dilatation of the calyces (Figure 5) [92–94].

CTU and MRI depict the disease more in detail with renal atrophy, hypertrohy of residual normal tissue (pseudotumor), irregular borders, cortical thinning, poor corticomedullary differentiation, parenchymal scars, calyceal distortion and clubbing (Figure 6). Moreover, contralateral renal hypertrophy, as a compensatory mechanism, can be observed [48].

RCS displays defects of 99mTc-DMSA uptake characteristic to renal scarring.

Renal needle biopsy is a gold standart for diagnosing glomerulonephritis (GN). However, radiologic imaging is useful prior to biopsy.

Enlarged kidneys with either reduced or increased visibility of pyramids can be seen on CUS. Echogenicity of the renal parenchyma is associated to tubulointerstitial, not glomerular changes [95], [96]. In proliferative glomerulonephritis and interstitial nephritis tubulointerstitial compartment is severely damaged, therefore, renal cortex is hyperechoic. Contrary, renal parenchyma is normal in membranous glomerulonephritis, IgA nephropathy, minimal-change glomerulonpehritis and focal glomerulosclerosis at first. Nonetheless, progression of these diseases extend to the tubules and interstitium, hence, parenchyma gradually becomes hyperechoic [97]. In addition, CUS may demonstrate inhomogeneous renal sinus with poor renal sinus-parenchymal differentiation.

Doppler US allows to assess renal function precisely in patients with chronic GN. Several studies show that resistive index (RI) correlates to the extent of arteriolosclerosis, glomerulosclerosis and interstitial fibrosis [98, 99]. T.Yura et al. also established correlation between creatinine clearance and both peak systolic velocity and end-di-

astolic velocity. Moreover, inverse correlation between creatinine clearance, RI and pulsatility index (PI) was determined in their study [100]. RI usually increases only in acute crescentic and proliferative glomerulonephritis and diseases of the tubulointerstitial compartment. However, these findings are not specific to GN.

CEUS benefits in diagnosing early glomerular disease. According to M. Nestola et al., histological activity of GN correlates with persistence of contrasts material signal in the wash-out phase. Slower contrast agent wash-out purposes disturbed glomerular perfusion in early GN [101].

A recent study concluded that a quantitative elastography technique can also contribute to the early diagnosis of GN. Shear wave based elastography point quantification (ElastPQ) determines renal cortical stifness, which is higher in pediatric patients with glomerular disease [102]. Nonetheless, further research is needed.

MRI is another imaging modality that is helpful in diagnosis and follow-up of patients with chronic GN. Diffusion tensor imaging (DTI) allows to evaluate renal function and the degree of histopathological abnormalities. Glomerulosclerosis and tubulointerstitial fibrosis reduces parenchymal perfusion, leading to decreased diffusivity. These histopathological changes may also influence diffusion direction along the tubules. As a result, ADC and fractional anisotropy (FA) values decreases with increased chronic GN stages. Furthermore, corticomedullary differentiation is poorer with each stage, as shown in Figure 7 [103].

Contrast-enhanced MRI may differentiate active and treatable glomerular disease between sclerotic ones. In cases of chronic GN, ultrasmall superparamagnetic iron oxide particles (USPIO) are used as a contrast agent. USPIO displays cortical macrophage infiltration, corresponding to inflammatory renal regions. Due to accumulation of iron particles in mononuclear cells, MRI demonstrates diffusely decreased enhancement of renal parenchyma on T2W images after USPIO administration [104].

In conclusion, radiology plays an important role in diagnosis of inflammatory renal diseases. Imaging allows to identify renal abnormalities and differentiate between a few feasible pathologies. It may also evaluate the activity of the disease. Moreover, it can assess sequelae, such as renal scarring and decreased renal function. Although US is the first-line imaging modality in most of the cases, CT is usually referred to be the most informative one. MRI is a radiation-free alternative and is not routinely used. Nonetheless, it is relevant in the early detection of glomerulonephritis. In order to identify the sequelae of these diseases, RCS can be beneficial, especially in the pediatric population.

REFERENCES

1. Koufadaki AM, Karavanaki KA, Soldatou, Tsentidis CH, Sourani MP, Sdogou T, Haliotis FA, Stefanidis. Clinical and laboratory indices of severe renal lesions in children with febrile urinary tract infection. Acta Paediatr 2014; 103: e404–e409.

2. Kirac Y, Bilen S, Duranay M. Comparison of laboratory findings in patients with glomerulonephritis classified according to histopathologic diagnosis. Minerva Medica 2014; 105: 149-156.

3. Al Turk AA, Estiverne C, Agrawal PR, Michaud JM. Trends and outcomes of the use of percutaneous native kidney biopsy in the United States: 5-year data analysis of the Nationwide Inpatient Sample. Clin Kidney J 2017; 11(3): 330–336.

4. Nickavar A, Safaeian B, Biglari abhari M. Radiologic and clinical evaluation of children with first febrile urinary tract infection. Int J Pediatr Adolesc Med 2015; 2: 24–28.

5. Yoo JM, Koh JS, Han CH, Lee SL, Ha U-S, Kang SH, Yung YS, Lee YS. Diagnosing acute pyelonephritis with CT, 99mTc-DMSA SPECT, and Doppler ultrasound: a comparative study. Korean J Urol 2010; 51: 260–265.

6. Nikolic O, Stojanovic S, Till V, Basta-Nikolic M, Petrovic K, Vucaj-Cirilovic V. Multislice computed tomography urography in the diagnosis of urinary tract diseases. Vojnosanit Pregl 2011; 68(5): 417–422.

7. Lee JKT, McClennan BL, Melson GL, Stanley RJ. Acute focal bacterial nephritis: emphasis on grey scale sonography and computed tomography. AJR 1980; 135: 87-92.

8. Venkatesh L, Hanumegowda RK. Acute pyelonephritis - correlation of clinical parameter with radiological imaging abnormalities. J Clin Diagnostic Res 2017; 11(6): TC15-TC18.

9. Piccoli GB, Colla L, Burdese M, Marcuccio C, Mezza E, Maass J, Picciotto G, Sargiotto A, L. Besso, Magnano E et al. Development of kidney scars after acute uncomplicated pyelonephritis: relationship with clinical, laboratory and imaging data at diagnosis. World J Urol 2006; 24: 66–73.

10. Cheng CH, Tsau YK, Chen SY, Lin TY. Clinical courses of children with acute lobar nephronia correlated with computed tomographic patterns. Pediatr Infect Dis J. 2009; 28: 300–303.

11. Lim SK, Ng FC. Acute pyelonephritis and renal abscesses in adults-correlating clinical parameters with radiological (computer tomography) severity. Ann Acad Med Singapore 2011; 40: 407–413.

12. Lavocat MP, Granjon D, Allard D, Gay C, Freycon MT, Dubois F. Imaging of pyelonephritis. Pediatr Radiol 1997; 27: 159–165.

13. Majd M, Rushton HG, Chandra R, Andrich MP, Tardif CP, Rashti F. Technetium-99m-DMSA renal cortical scintigraphy to detect experimental acute pyelonephritis in piglets: comparison of planar (pinhole) and SPECT imaging. J Nucl Med 1996; 37: 1731–1734.

14. Sty JR, Wells RG, Starshak RJ, Schroeder BA. Imaging in acute renal infection in children. AJR 1987; 148: 471–477.

15. Kovanlikaya A, Okkay N, Cakmakci H, Ozdogan O, Degirmenci B, Kavukcu S. Comparison of MRI and renal cortical scintigraphy findings in childhood acute pyelonephritis: preliminary experience. Eur J Radiol 2004; 49: 76–80.

16. Bosakova A, Salounova D, Havelka J, Kraft O, Sirucek P, Kocvara R, Hladik M. Diffusion-weighted magnetic resonance imaging is more sensitive than dimercaptosuccinic acid scintigraphy in detecting parenchymal lesions in children with acute pyelonephritis: a prospective study. J Pediatr Urol 2018; 14: 269. e1-269.e7.

17. Kavanagh EC, Ryan S, Awan A, McCourbrey S, O'Connor R, Donoghue V. Can MRI replace DMSA in the detection of renal parenchymal defects in children with urinary tract infections? Pediatr Radiol 2005; 35: 275–281.

18. Brenner M, Bonta D, Eslamy H, Ziessman HA. Comparison of 99mTc-DMSA dual-head SPECT versus high-resolution parallel-hole planar imaging for the detection of renal cortical defects. AJR 2009; 193: 333–337.

19. Liu XQ, Wang CC, Liu YB, Liu K. Renal and perinephric abscesses in West China Hospital: 10-year retrospective-descriptive study. World J Nephrol 2016; 5(1): 108-114.

20. Manjon CC, Sanchez AT, Lara JDP, Silva VM, Betriu GC, Sanchez AR, Penalver CG, Galvis OL. Retroperitoneal abscesses - analysis of a series of 66 cases. Scand J Urol Nephrol 2003; 37: 139–144.

21. Rollino C, Beltrame G, Ferro M, Quattrocchio G, Sandrone M, Quarello F. Acute pyelonephritis in adults: a case series of 223 patients. Nephrol Dial Transplant 2012; 27: 3488–3493.

22. Tsu JHL, Chan CK, Chu RWH, Law IC, Kong CK, Liu PL, Cheung FK, Yiu MK. Emphysematous pyelonephritis: an 8-year retrospective review across four acute hospitals. Asian J Surg 2013; 36: 121–125.

23. Wang JM, Lim HK, Pang KK. Emphysematous pyelonephritis. Scand J Urol Nephrol 2007; 41: 223–229.

24. Kim DS, Woesner ME, Howard TF, Olson LK. Emphysematous pyelonephritis demonstrated by computed tomography. AJR 1979; 132: 287–288.

25. Czaja CA, Scholes D, Hooton TM, Stamm WE. Population-based epidemiologic analysis of acute pyelonephritis. Clin Infect Dis 2007; 45: 273–280.

26. Ki M, Park T, Choi B, Foxman B. The epidemiology of acute pyelonephritis in South Korea, 1997-1999. Am J Epidemiol 2004; 160(10): 985–993.

27. Lee YJ, Cho S, Kim SR. Unilateral and bilateral acute pyelonephritis: differences in clinical presentation, progress and outcome. Postgrad Med J 2014; 90: 80–85.

28. Kawashima A, Sandler CM, Goldman SM, Raval BK, Fishman EK. CT of renal inflammatory disease. Radiographics 1997; 17(4): 851-866.

29. Craig WD, Wagner BJ, Travis MD. Pyelonephritis: radiologic-pathologic review. RadioGraphics 2008; 28: 255–277.

30. Dinkel E, Orth S, Dittrich, M, Schulte-Wissermann H. Renal sonography in the differentiation of upper from lower urinary tract infection. AJR, 1986; 146: 775–780.

31. Farmer KD, Gellett LR, Dubbins PA. The sonographic appearance of acute focal pyelonephritis 8 years experience. Clin Radiol 2002; 57: 483–487.

32. Rigsby CM, Rosenfield AT, Glickman MG, Hodson J. Hemorrhagic focal bacterial nephritis: findings on gray-scale sonography and CT. AJR 1986; 146: 1173–1177.

33. Kao HW, Wu CJ. Ultrasound of renal infectious disease. J Med Ultrasound 2008; 16(2): 113–122.

34. Kim B, Lim HK, Choi MH, Woo JY, Ryu J, Kim S, Peck KR. Detection of parenchymal abnormalities in acute pyelonephritis by pulse inversion harmonic imaging with or without microbubble ultrasonographic contrast agent: correlation with computed tomography. J Ultrasound Med 2001; 20: 5–14

35. Ehsanipour F, Gharouni M, Rafati AH, Ardalan M, Bodaghi N, Otoukesh H. Risk factors of renal scars in children with acute

pyelonephritis. Braz J Infect Dis 2012; 16(1): 15–18.

36. Chung EM, Soderlund KA, Fagen KE. Imaging of the pediatric urinary system. Radiol Clin N Am 2017; 55: 337–357.

37. Hamoui N, Hagerty JA, Maizels M, Yerkes EB, Chaviano A, Shore R, Kaplan WE, Cheng EY. Ultrasound fails to delineate significant renal pathology in children with urinary tract infections: a case for dimercapto-succinic acid scintigraphy. J Urol 2008; 180: 1639–1642.

38. Gulati M, Cheng J, Loo JT, Skalski M, Malhi H, Duddalwar V. Pictorial review: renal ultrasound. Clin Imaging 2018; 51: 133–154.

39. Dacher JN, Pfister C, Monroc M, Eurin D, Le Dosseur P. Power Doppler sonographic pattern of acute pyelonephritis. AJR 1996; 166: 1451-1455.

40. Winters WD. Power Doppler sonographic evaluation of acute pyelonephritis in children. J Ultrasound Med 1996; 15: 91-96.

41. Rathaus V, Werner M. Acute focal nephritis: its true sonographic face. Isr Med Assoc J 2007; 9: 729–731.

42. Uehling DT, Hahnfeld LE, Scanlan KA. Urinary tract abnormalities in children with acute focal bacterial nephritis. BJU Int 2000; 85: 885–888.

43. Fontanilla T, Minaya J, Cortes C, Hernando CG, Aranguena RP, Arriaga J, Carmona MS, Alcolado A. Acute complicated pyelonephritis: contrast-enhanced ultrasound. Abdom Imaging 2012; 37: 639–646.

44. Granata A, Andrulli S, Fiorini F, Basile A, Logias F, Figuera M, Sicurezza E, Gallieni M, Fiore CE. Diagnosis of acute pyelonephritis by contrast-enhanced ultrasonography in kidney transplant patients. Nephrol Dial Transplant 2011; 26: 715–720.

45. Mitterberger M, Pinggera GM, Colleselli D, Batsch G, Strasser H, Steppan I, Pallwein L, Friedrich A, Gradl J, Frauscher F. Acute pyelonephritis: comparison of diagnosis with computed tomography and contrast-enhanced ultrasonography. BJU Int 2008; 101: 341–344.

46. Bertolotto M, Bucci S, Valentino M, Curro F, Sachs C, Cova MA. Contrast-enhanced ultrasound for characterizing renal masses. Eur J Radiol 2018; 105: 41–48.

47. Ifergan J, Pommier R, Brion MC, Glas L, Rocher L, Bellin MF. Imaging in upper urinary tract infections. Diagn Interv Imaging 2012; 93: 509–519.

48. Quaia E, Reiser MF, Kauczor HU, Gricak H, Knauth M. Radiological imaging of the kidney. 2nd ed. Berlin, Germany: Springer; 2014.

49. El-Merhi F, Mohamad M, Haydar A, Naffaa L, Nasr R, Deeb IAS, Hamieh N, Tayara Z, Saade C. Qualitative and quantitative radiological analysis of non-contrast CT is a strong indicator in patients with acute pyelonephritis. Am J Emerg Med 2018; 36: 589–593.

50. Gold RP, McClennan BL, Rottenberg RR. CT appearance of acute inflammatory disease of the renal interstitium. AJR 1983; 141: 343–349.

51. Campos-Franco J, Macia C, Huelga E, Diaz-Louzao C, Gude F, Alende R, Gonzalez-Quintela A. Acute focal bacterial nephritis in a cohort of hospitalized adult patients with acute pyelonephritis. Assessment of risk factors and a predictive model. Eur J Intern Med 2017; 39: 69–74.

52. Hoddick W, Jeffrey RB, Goldberg HI, Federle MP, Laing FC. CT and sonography of severe renal and perirenal infections. AJR 1983; 140: 517-520.

53. Saunders HS, Dyer RB, Shifrin RY, Scharling ES, Bechtold RE, Zagoria RJ. The CT nephrogram: implications for evaluation of urinary tract disease. RadioGraphics 1995; 15(5): 1069–1085.

54. Yu M, Robinson K, Siegel C, Menias C. Complicated genitourinary tract infections and mimics. Curr Probl Diagn Radiol 2017; 46: 74–83.

55. De Pascale A, Piccoli GB, Priola SM, Rognone D, Consiglio V, Garetto I, Rizzo L, Veltri A. Diffusion-weighted magnetic resonance imaging: new perspectives in the diagnostic pathway of non-complicated acute pyelonephritis. Eur Radiol 2013; 23: 3077–3086.

56. Martina MC, Campanino PP, Caraffo F, Marcuccio C, Gunetti F, Colla L, Cassinis MC, Gandini G. Dynamic magnetic resonance imaging in acute pyelonephritis. Radiol Med 2010; 115: 287–300.

57. Vivier PH, Sallem A, Beurdeley M, Lim RP, Leroux J, Caudron J, Coudray C, Liard A, Michelet I, Dacher JN. MRI and suspected acute pyelonephritis in children: comparison of diffusion-weighted imaging with gadolinium-enhanced T1-weighted imaging. Eur Radiol 2014; 24(1): 19–25.

58. Aoyagi J, Odaka J, Kuroiwa Y, Nakashima N, Ito T, Saito T, Kanai T, Yamagata T, Momoi MY. Utility of non-enhanced magnetic resonance imaging to detect acute pyelonephritis. Pediatr Int 2014; 56: e4-e6.

59. Reuther G, Kiefer B, Wandl E. Visualization of urinary tract dilatation: value of single-shot MR urography. Eur Radiol 1997; 7: 1276–1281.

60. Vegar-Zubovic S, Kristic S, Lincender L. Magnetic resonance urography in children - when and why? Radiol Oncol 2011; 45(3): 174–179.

61. Boss A, Martirosian P, Fuchs J, Obermayer F, Tsiflikas I, Schick F, Schafer JF. Dynamic MR urography in children with uropathic disease with a combined 2D and 3D acquisition protocol-comparison with MAG3 scintigraphy. Br J Radiol 2014; 87: 20140426.

62. McDaniel BB, Jones RA, Scherz H, Kirsch AJ, Little SB, Grattan-Smith JD. Dynamic contrast-enhanced MR urography in the evaluation of pediatric hydronephrosis: part 2, anatomic and functional assessment of uteropelvic junction obstruction. AJR 2005; 185: 1608–1614.

63. Ilyas M, Mastin ST, Richard GA. Age-related radiological imaging in children with acute pyelonephritis. Pediatr Nephrol 2002; 17: 30–34.

64. American academy of pediatrics. Urinary tract infection: clinical practice guideline for the diagnosis and management of the initial UTI in febrile infants and children 2 to 24 months. Pediatrics 2011; 128(3): 595–610

65. Piepsz A, Colarinha P, Gordon I, Hahn K, Olivier P, Roca I, Sixt R, van Velzen J. Revised guidelines on 99mTc-DMSA scintigraphy in children. Eur J Nucl Med 2009; 28(3): BP37-41.

66. Araujo CB, Barroso JR U, Barroso VA, Vinhaes AJ, Jacobino M, Calado A, Filho MZ. Comparative study between intravenous urography and renal scintigraphy with DMSA for the diagnosis of renal scars in children with vesicoureteral reflux. Int Braz J Urol 2003; 29(6): 535–539.

67. Raz R, Sakran W, Chazan B, Colodner R, Kunin C. Long-term follow-up of women hospitalized for acute pyelonephritis. Clin Infect Dis 2003; 37: 1014–1020.

68. Faust WC, Diaz M, Pohl HG. Incidence of post-pyelonephritic renal scarring: a meta-analysis of the dimercapto-succinic acid literature. J Urol 2009; 181: 290–298.

69. Hitzel A, Liard A, Vera P, Manrique A, Menard JF, Dacher JN.

Color and power Doppler sonography versus DMSA scintigraphy in acute pyelonephritis and in prediction of renal scarring. J Nucl Med 2002; 43(1): 27–32

70. Supavekin S, Surapaitoolkorn W, Pravisithikul N, Kutanavanishapong S, Chiewvit S. The role of DMSA renal scintigraphy in the first episode of urinary tract infection in childhood. Ann Nucl Med 2013; 27: 170–176.

71. Lee BE, Seol HY, Kim TK, Seong EY, Song SH, Lee DW, Lee SB, Kwak IS. Recent clinical overview of renal and perirenal abscesses in 56 consecutive cases. Korean J Intern Med 2008; 23(3): 140–148.

72. Piccoli G, Consiglio V, Deagostini MC, Serra M, Biolcati M, Ragni F, Biglino A, De Pascale A, Frascisco MF, Veltri A et al. The clinical and imaging presentation of acute "non complicated" pyelonephritis: a new profile for an ancient disease. BMC Nephrol 2011; 12: 68.

73. Sato M, Suzuki S, Shimada S, Yamamoto S, Taketazu G, Mukai T, Taketazu M, Sakata H, Oki J. Serial sonographic findings during progression from acute pyelonephritis to renal abscess: a rare case report. CEN Case Reports 2017; 6: 8–21.

74. Morehouse HT, Weiner SN, Hoffman C. Imaging in inflammatory disease of the kidney. AJR 1984; 143: 135–141.

75. Zissin R, Gayer G, Kots E, Werner M, Shapiro-Feinberg M, Hertz M. Iliopsoas abscess: a report of 24 patients diagnosed by CT. Abdom Imaging 2001; 26: 533–539.

76. Brown ED, Brown JJ, Kettritz U, Shoenut JP, Semelka RC. Renal abscesses: appearance on gadolinium-enhanced magnetic resonance images. Abdom Imaging 1996; 176: 172–176.

77. Gerzof SG, Robbins AH, Birkett DH. Computed tomography in the diagnosis and management of abdominal abscesses. Abdom Imaging 1978; 3: 287–294.

78. Hoffer FA, Shamberger RC, Teele RL. Ilio-psoas abscess: diagnosis and management. Pediatr Radiol 1987; 17: 23–27.

79. Unal O, Koparan HI, Avcu S, Kalender AM, Kisli E. The diagnostic value of diffusion-weighted magnetic resonance imaging in soft tissue abscesses. Eur J Radiol 2011; 77: 490–494.

80. Olvera-Posada D, Armengod-Fischer G, Vazquez-Lavista LG, Maldonado-Avila M, Rosa-Nava E, Manzanilla-Garcia H, Castillejos-Molina RA, Mendez-Probst CE, Sotomayor M, Feria-Bernal G et al. Emphysematous pyelonephritis: multicenter clinical and therapeutic experience in Mexico. Urology 2014; 83(6): 1280–1284.

81. Lu YC, Chiang BJ, Pong YH, Huang KH, Hsueh PR, Huang CY, Pu YS. Predictors of failure of conservative treatment among patients with emphysematous pyelonephritis. BMC Infect Dis 2014; 14: 418.

82. Sanford TH, Myers F, Chi T, Bagga HS, Taylor AG, Stoller ML. Emphysematous pyelonephritis: the impact of urolithiasis on disease severity. Transl Androl Urol 2016; 5(5): 774–779.

83. Bjurlin MA, Hurley SD, Kim DY, Cohn MR, Jordan MD, Kim R, Divakaruni N, Hollowell CMP. Clinical outcomes of nonoperative management in emphysematous urinary tract infections. Urology 2012; 79(6): 1281–1285.

84. Aswathaman K, Gopalakrishnan G, Gnanaraj L, Chacko NK, Kekre NS, Devasia A. Emphysematous pyelonephritis: outcome of conservative management. Urology 2008; 71 (6): 1007–1009.

85. Allen HA, Walsh JW, Brewer WH, Vick CW, Haynes JW. Sonography of emphysematous pyelonephritis. J Ultrasound Med 1984; 3: 533–537.

86. Narlawar RS, Raut AA, Nagar A, Hira P, Hanchate V, Asrani A. Imaging features and guided drainage in emphysematous pyelonephritis: a study of 11 cases. Clin Radiol 2004; 59: 192–197.

87. Wan YL, Lee TY, Bullard MJ, Tsai CC. Acute gas-producing bacterial renal infection: correlation between imaging findings and clinical outcome. Radiology 1996; 198(2): 433-438.

88. Huang JJ, Tseng CC. Emphysematous pyelonephritis. Clinicoradiological classification, management, prognosis and pathogenesis. Arch Intern Med 2000; 160(6): 797-805.

89. Kua CH, Abdul Aziz YF. Air in the kidney: between emphysematous pyelitis and pyelonephritis. Biomed Imaging Interv J 2008; 4(3): e24.

90. Hodson CJ. The radiological diagnosis of pyelonephritis. Proc R Soc Med 1959; 52: 669–672.

91. Hodson CJ. The radiology of chronic pyelonephritis. Postgrad Med J 1965; 41: 477–480.

92. Kay CJ, Rosenfield AT, Taylor KJW, Rosenberg MA. Ultrasonic characteristics of chronic atrophic pyelonephritis. AJR 1979; 132 : 47–49.

93. Tchakarski V, Mushmov D. Potentials of ultrasonography for early diagnosis of primary chronic pyelonephritis. Int Urol Nephrol 1988; 20(6): 665–667.

94. Schneider M, Becker JA, Staiano S, Campos E. Sonographic-radiographic renal and perirenal correlation infections. AJR 1976; 127: 1007–1014.

95. Rosenfield T, Siegel NJ. Renal parenchymal disease: histopathologic-sonographic correlation. AJR 1981; 137: 793-798.

96. Rosenfield AT. Ultrasound evaluation of renal parenchymal disease and hydronephrosis. Urol Radiol 1982; 4: 125–133.

97. Quaia E, Bertolotto M. Renal parenchymal diseases: is characterization feasible with ultrasound? Eur Radiol 2002; 12: 2006–2020.

98. Mostbeck GH, Kain R, Mallek R, Derfler K, Walter R, Havelec L, Tscholakoff D. Duplex Doppler sonography in renal parenchymal disease. J Ultrasound Med 1991; 10: 189–194.

99. Gigante A, Barbano B, Di Mario F, Rosato E, Simonelli M, Rocca AR, Conti F, Ceccarelli F, Giannakakis K, Valesini G et al. Renal parenchymal resistance in patients with biopsy proven glomerulonephritis: correlation with histological findings. Int J Immunopathol Pharmacol 2016; 29(3): 469–474.

100. Yura T, Yuasa S, Sumikura T, Takahashi N, Aono M, Kunimune Y, Fujioka H, Miki S, Takamitsu Y, Matsuo H. Doppler sonographic measurement of phasic renal artery blood flow velocity in patients with chronic glomerulonephritis. J Ultrasound Med 1993; 4: 215–219.

101. Nestola M, De Matthaeis N, Ferraro PM, Fuso P, Constanzi S, Zannoni GF, Pizzolante F, Quadra SV, Gambaro G, Rapaccini GL. Contrast-enhanced ultrasonography in chronic glomerulonephritides: correlation with histological parameters of disease activity. J Ultrasound 2018; 21: 81–87.

102. Xu B, Jiang G, Ye J, He J, Xie W. Research on pediatric glomerular disease and normal kidney with shear wave based elastography point quantification. Jpn J Radiol 2016; 34: 738–746.

103. Feng Q, Ma Z, Wu J, Fang W. DTI for the assessment of disease stage in patients with glomerulonephritis - correlation with renal histology. Eur Radiol 2015; 25: 92–98.

104. Hauger O, Grenier N, Deminere C, Lasseur C, Delmas Y, Merville P, Combe C. USPIO-enhanced MR imaging of macrophage infiltration in native and transplanted kidneys: initial results in humans. Eur Radiol 2007; 17: 2898–2907.